Winter 12-2003

Low temperature (2K - 20K) heat capacity determination of a polycrystalline zirconium oxide (ZrO) based material containing calcium (Ca) and europium (Eu)

Watasha M. Wade

Low Temperature (2 K – 20 K) Heat Capacity Determination of a Polycrystalline Zirconium Oxide (ZrO) Based Material Containing Calcium (Ca) and Europium (Eu)

A Thesis

Presented to

the Faculty of the Graduate School

Southern University

In Partial Fulfillment

of the Requirements for the Degree

Master of Science

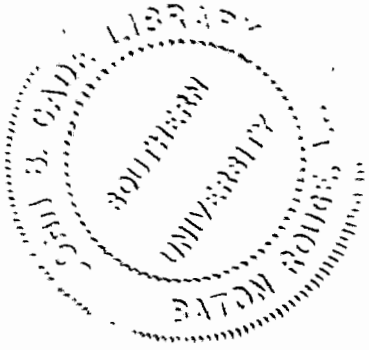

by

Watasha M. Wade
December, 2003

The Graduate School

Southern University
Baton Rouge, Louisiana

CERTIFICATE OF APPROVAL

MASTER'S THESIS

This is to certify that the Master's Thesis of

Watasha M. Wade

has been approved by the examining committee for the thesis requirement for the Master of Science degree in Physics, December, 2003

Chair of Committee:
Laurence L. Henry, Ph.D.

Committee Member:
Pradeep Bhattacharya, Ph.D.

Committee Member:
Diola Bagayoko, Ph.D.

Committee Member:
Stephen C. McGuire, Ph.D.

Chair of the Department of Physics:
Stephen C. McGuire, Ph.D.

Dean of the College of Sciences:
Robert H. Miller, Ph.D.

Dean of the Graduate School:
James Llorens, Ph.D.

Ms. Wade supported by the M.S. Physics Program, Southern University and A & M College, Baton Rouge, LA while she worked towards her degree. Support for the sample fabrication component of the research was under NASA Partnership Grant # NAG8-1627.

Low Temperature (2 K – 20 K) Heat Capacity Determination of a Polycrystalline Zirconium Oxide (ZrO) Based Material Containing Calcium (Ca) and Europium (Eu)

An Abstract of a Thesis

Presented to

the Faculty of the Graduate School

Southern University

In Partial Fulfillment

of the Requirements for the Degree

Master of Science

---

by

Watasha M. Wade
December, 2003

Abstract

The calorimetric properties of a CaEuZrO based sample, synthesized by a solid-state reaction process in the Electron Transport and Magnetic Properties of Materials (ETMPM) lab, are investigated by analyzing low temperature (2 – 20 K) heat capacity data. The total heat capacity of a material may be expressed as $C = C_{elec} + C_{ph} + C_{nuc} + C_{mag} + C_i$. In mathematical terms, it may be expressed as $C = \gamma T + \alpha T^3 + A_n T^{-2} + C_i$. In this equation, the term γT is the electronic heat capacity, αT^3 is the lattice or phonon heat capacity, $A_n T^{-2}$ is the nuclear heat capacity and C_i represents any other heat capacity contributors that may be present. The various contributors may be identified based on their distinct temperature dependence in different temperature ranges. In the study, previously collected heat capacity data for the sample is analyzed. Estimates for the lattice and electronic coefficients were determined to be $\alpha = 1 \times 10^{-6}$ J/g-K^4 and $\gamma = 2 \times 10^{-7}$ J/g-K^2, respectively. Thus, the lattice heat capacity is dominant in the temperature range from 2 - 20 K.

Acknowledgements

First, the author would like to thank God for his many blessings! She would also like to thank her family and friends for their support. A special thanks goes to Tiffiny for her many encouraging words. A very special "thank you" is extended to James for believing in me and supporting me every step of the way.

The author would also like to recognize the Timbuktu Academy for its mentoring and financial support throughout her undergraduate studies. The M.S. Physics Program funded her graduate studies. A special thanks is extended to Dr. Diola Bagayoko for his continued support, guidance, and mentoring throughout the author's academic career.

A personal thanks goes to the author's research advisor, Dr. Laurence L. Henry, for his patience and support throughout her thesis preparation. The author would also like to thank the Electron Transport and Magnetic Properties of Materials (ETMPM) group for their assistance in the material fabrication and data collection phases of the study.

Last, but not least, the author would like to thank everyone who played any role in helping her to achieve this goal.

Table of Contents

List of Figures

List of Tables

Recently, the group of Jose, James, John, Divakar and Koshy reported the first synthesis of a new complex perovskite ceramic oxide material, barium europium zirconium oxide ($Ba_2EuZrO_{5.5}$), by a solid-state reaction process[1]. The material was developed for its potential use as a substrate for $YBa_2Cu_3O_{7-\delta}$ (YBCO) and Bi (2223) superconductors[1-4]. The material was to meet several requirements, namely, being chemically non-reactive with YBCO and Bi (2223) superconductors and having a low dielectric constant and loss factor to make it suitable for microwave applications[1-4]. X-ray diffraction studies and resistance measurements revealed that both YBCO and Bi (2223) superconductors did not show any detectable chemical reaction with $Ba_2EuZrO_{5.5}$, even under extreme processing conditions[5]. Studies also showed that the dielectric constant and loss factor of $Ba_2EuZrO_{5.5}$ were in a range suitable for the use of the material as a substrate for microwave applications[5]. Throughout the research, the group synthesized many different complex perovskite ceramic oxides, namely $Ba_2AZO_{5.5}$, where A is Eu, Dy, Y or La, and Z is Zr, Hf or Sn[1-4]. Thus, it was shown that these new materials could serve as substrates for both $YBa_2Cu_3O_{7-\delta}$ and Bismuth (2223) superconductors. Upon learning of the synthesis of this new material, the Electron Transport and Magnetic Properties of Materials (ETMPM) group attempted to synthesize the material.

A previous student, using a conventional solid-state reaction process, fabricated the material in the ETMPM lab. The material was characterized by x-ray diffraction and shown to have a perovskite structure. After this attempt, the group attempted to synthesize a similar complex perovskite ceramic oxide by substituting barium with calcium. The motivation was to examine the effects of replacing the barium atoms with atoms of another alkaline earth metal which has a smaller atomic radius and better electrical conductivity. The atomic radii of barium and calcium are 2.28 Å and 2.23 Å, respectively. The electrical conductivity of barium and calcium are 0.030 $10^6/cm\Omega$ and 0.298 $10^6/cm\Omega$, respectively. The new material, $Ca_2EuZrO_{5.5}$ (nominal) was synthesized in air by a solid-state reaction process. XRD data were collected on the sample; however, a chemical composition determination was not carried out because the material had disintegrated to powder form by the time this procedure was to have been carried out. The group then proceeded to study the calorimetric properties of the new material. Heat capacity data obtained from the $Ca_2EuZrO_{5.5}$ (nominal) attempt were investigated. Since a composition determination could not be performed on the material, we do not know that the actual material is the intended material. Hence, we will refer to the material that was made as a polycrystalline ceramic oxide (PCO) sample instead of $Ca_2EuZrO_{5.5}$ (nominal). The abbreviation PCO will be used to refer to the sample in the remaining of this thesis.

Calorimetry measurements are an important tool in gaining knowledge about the properties of materials that involve changes in the internal energy, such as phase transitions. Phase transitions give valuable information about the structural, electronic and magnetic ordering that takes place within a material. One of the best tools for investigating phase transition is heat capacity data analysis. It can be used to obtain estimates of values for specific parameters such as the Debye temperature of a material. The Debye temperature is an indication of the bond strength within the material. For example, a material such as diamond has a high Debye temperature and is very hard to break, however, a material with a low Debye temperature such as chalk, breaks easily. Complete pictures about the internal energy contributors of a material can be found by separating the heat capacity data into its constituent components.

The objective of the study is to analyze heat capacity data from the PCO sample and to extract the various heat capacity contributors. This information is useful in understanding the properties of the material.

The heat capacity of a material is composed of the lattice, electronic, nuclear and magnetic heat capacities, in addition to that from other contributors. The various contributors may be identified based on their distinct temperature dependence in different temperature ranges. In this study, the heat capacity data for the sample is analyzed and the coefficients of the electronic and lattice terms are calculated. An initial assumption is made that the nuclear contribution is minimal compared to the lattice and electronic contributions. This is reasonable

The heat capacity C of a material can be expressed as[8]

$$C = \Delta Q/\Delta T, \tag{2.1}$$

where ΔQ is the amount of heat applied to a given amount of the material and ΔT is the resulting temperature change[8]. It is an extensive quantity, i.e., it is dependent on the amount of material involved in the heating.

The specific heat c is the amount of heat required to raise the temperature of a unit mass of a material by a unit degree of temperature[8]. Although directly related to the heat capacity, the specific heat is an intrinsic property, i.e., it is independent of the amount of material involved in the heating. c is unique for each material and can be expressed as[8]

$$c = \Delta Q/(m\Delta T), \tag{2.2}$$

where m is the mass of the sample. The relationship between c and C is

$$c = C/m. \tag{2.3}$$

The total heat capacity C of a material consists of various contributors including the lattice or phonon heat capacity (C_{ph}), the electronic heat capacity (C_{elec}), the nuclear heat capacity (C_{nuc}), and in the case of magnetic materials, the magnetic heat capacity (C_{mag})[8]. Thus, the total heat capacity of a material can be expressed as

$$C = C_{ph} + C_{elec} + C_{nuc} + C_{mag} + C_i, \tag{2.4}$$

where C_i represents any additional contributors[8]. The first three terms can be determined independently using their relative strengths in various temperature ranges due to their difference temperature dependencies.

The electronic heat capacity is given by

$$C_{elec} = \gamma T, \tag{2.5}$$

the lattice heat capacity is given by

$$C_{ph} = \alpha T^3 \tag{2.6}$$

and the nuclear heat capacity is given by

$$C_{nuc} = A_n T^{-2}, \tag{2.7}$$

where α, γ and A_n are constants to be determined and T is the temperature in degree Kelvin (°K). For ferromagnetic materials, the magnetic heat capacity (C_{mag}) has a $T^{3/2}$ dependence at low temperatures[6].

The electronic heat capacity is the heat capacity associated with the movement of free electrons through the material[8]. The coefficient γ is related to the electron density of states through the relation[7]

$$\gamma = (\pi^2/3)DOS(E_F)k^2_B, \tag{2.8}$$

where $DOS(E_F)$ is the electron density at the Fermi energy (E_F) and k_B is Boltzmann's constant. Using the electron density of states, the Fermi energy (E_F) can be calculated. And with the Fermi energy, the Fermi temperature (T_F) can be calculated. The Fermi energy is that of the highest occupied energy state. The Fermi temperature is the temperature above which the electrons behave like a

classical gas, and far below which the electrons approximate the ground states with small excitations at the Fermi level.

The lattice or phonon heat capacity is associated with the movement of atoms or ions at the lattice points. The coefficient α may be written as[8]

$$\alpha = (12rR\pi^4/5\theta^3_D). \tag{2.9}$$

where r is the number of atoms per molecule, R is the universal gas constant, and θ_D is the Debye temperature. The Debye temperature is related to the strength of the bonds within the material and is given by[8]

$$\theta_D = h\upsilon_D/k_B \tag{2.10}$$

where υ_D is the "cutoff" or maximum frequency of phonon or lattice vibrations[8]. The cutoff frequency corresponds to a minimum possible phonon wavelength of the same order as the lattice spacing[8].

The nuclear heat capacity is the heat capacity associated with the nuclear moments within the atom and has a $1/T^2$ dependence for temperatures larger than the nuclear splitting energy. The nuclear heat capacity is only observed at extremely low temperatures ($T < 2K$), which makes it difficult to determine experimentally.

The magnetic heat capacity is the heat capacity associated with the magnetic spin waves (magnons) in the material and depends on the magnetic configuration of the material[8]. For example, the magnon heat capacity of ferromagnets exhibits a $T^{3/2}$ dependence at low temperatures; however, antiferomagnets exhibit a T^3 temperature dependence[8].

Different theories have been used to describe the heat capacity. They include the Debye theory, the Einstein theory and the Dulong-Petit law. The Dulong Petit law gives a theoretical explanation for the heat capacity and is especially useful at high temperatures. In the high temperature limit the Dulong Petit law gives an estimate for the heat capacity as[8]

$$C = 3nR, \tag{2.11}$$

where n is the number of atoms per molecule in the sample, and R is the universal gas constant[8]. The Dulong-Petit Law is mostly applicable at high temperatures, since it does not agree well with the experimental data at low temperatures. At high temperatures, it agrees with both the Einstein and Debye models of a crystal lattice. The Einstein model is based on a very simple description of the movement of the lattice in the material. It suggests that all atoms in a lattice vibrate at the same frequency. The Einstein model leads to the Dulong-Petit value at high temperatures and shows how, at low temperatures, the quantization of lattice vibrations results in a reduction of the heat capacity[8]. Unfortunately, the Einstein model does not quite agree with experimental data at low temperatures. With the Einstein model as a base, the Debye model gives good results from low to high temperatures[8]. It assumes that low frequency vibrations are propagated throughout the material[8]. This theory suggests that the collective low-frequency oscillations of the solid should be applied even at high frequencies and the discrete nature of the atomic lattice should be taken into account by setting a minimum for the allowed wavelengths[8]. The minimum

wavelength corresponds to the cutoff frequency, υ_D[8]. This model is successful at high temperatures as well as at very low temperatures[8]. At high temperatures, it agrees well with the Einstein model and the Dulong-Petit law. At low temperatures, it agrees well with experimental data.

The heat capacity can be measured at constant volume or pressure. Both values are related through the relation[8]

$$C_p = C_v + [(\delta U/\delta V)_T + P]V\beta, \qquad (2.12)$$

where C_p is the heat capacity at constant pressure and C_v is the heat capacity at constant volume. P, V, T are the pressure, volume, and temperature, respectively. β is the coefficient of volume expansion and is given by[6]

$$\beta = (1/V)(\delta V/\delta T)_p. \qquad (2.13)$$

The values for β are of the order of $10^{-5}K^{-1}$, and for temperatures below 100K, the fractional change in the volume is on the order of $10^{-3}m^3$ or less[8]. Hence, for small sample and low temperatures, the second term in the equation for C_p is negligible, and $C_p \approx C_v$[8]. The sample size is of the order of mm^2 and it has a low mass (18 mg). Hence the $C_p \approx C_v$ approximation will be made throughout the thesis.

Chapter 3: Experimental

This chapter describes the experimental component of the research. Both, the sample synthesis and the heat capacity measurements were done in the ETMPM lab (by previous students). The author's responsibility has been to analyze the heat capacity data that were collected. Because the author was not involved in carrying out the experimental techniques on the sample, this chapter gives only a brief summary of the techniques as they relate to the sample and the heat capacity measurements. XRD data were also collected on the sample.

The sample used in the study had a mass of 18 mg and was fabricated in air using a solid-state reaction process. The parent stock (sample #80701) from which the sample was taken was created by mixing stoichiometric amounts of high purity starting compounds of $CaCO_3$, Eu_2O_3 and ZrO_2 and by sintering the mixture at different temperatures for various amounts of time. The samples were formed by pressing pieces of the parent stock into three pellets. The first pellet (1400/14), which is the focus of this study, was sintered at 1340° C for 14 hours. The compound intended to be synthesized was $Ca_2EuZrO_{5.5}$, however, the actual composition that resulted has not yet been determined. A composition determination was not performed because the sample has disintegrated and is back in the powder form. An investigation of the x-ray diffraction data to look for unreacted remnants of the starting compounds showed that none remained following the fabrication process. Analysis of x-ray data also showed that the

material does not have a typical perovskite structure. The x-ray data are is shown in Figure 3.1. Figure 3.2 shows data from a typical perovskite material.

Figure 3.1: x-ray 80701

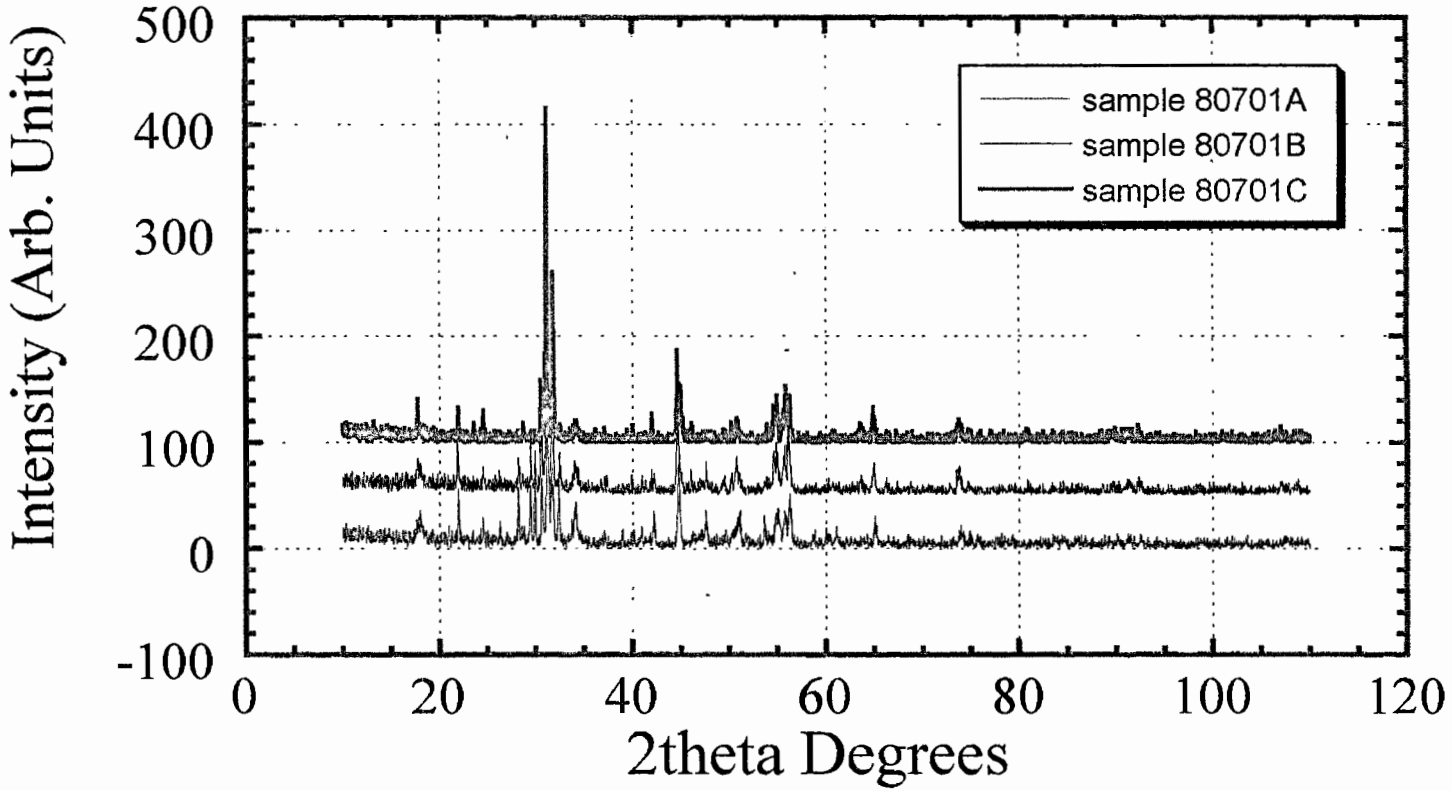

Figure 3.2 Plot of Intensity vs. 2 θ of the x-ray diffraction data for a typical perovskite material

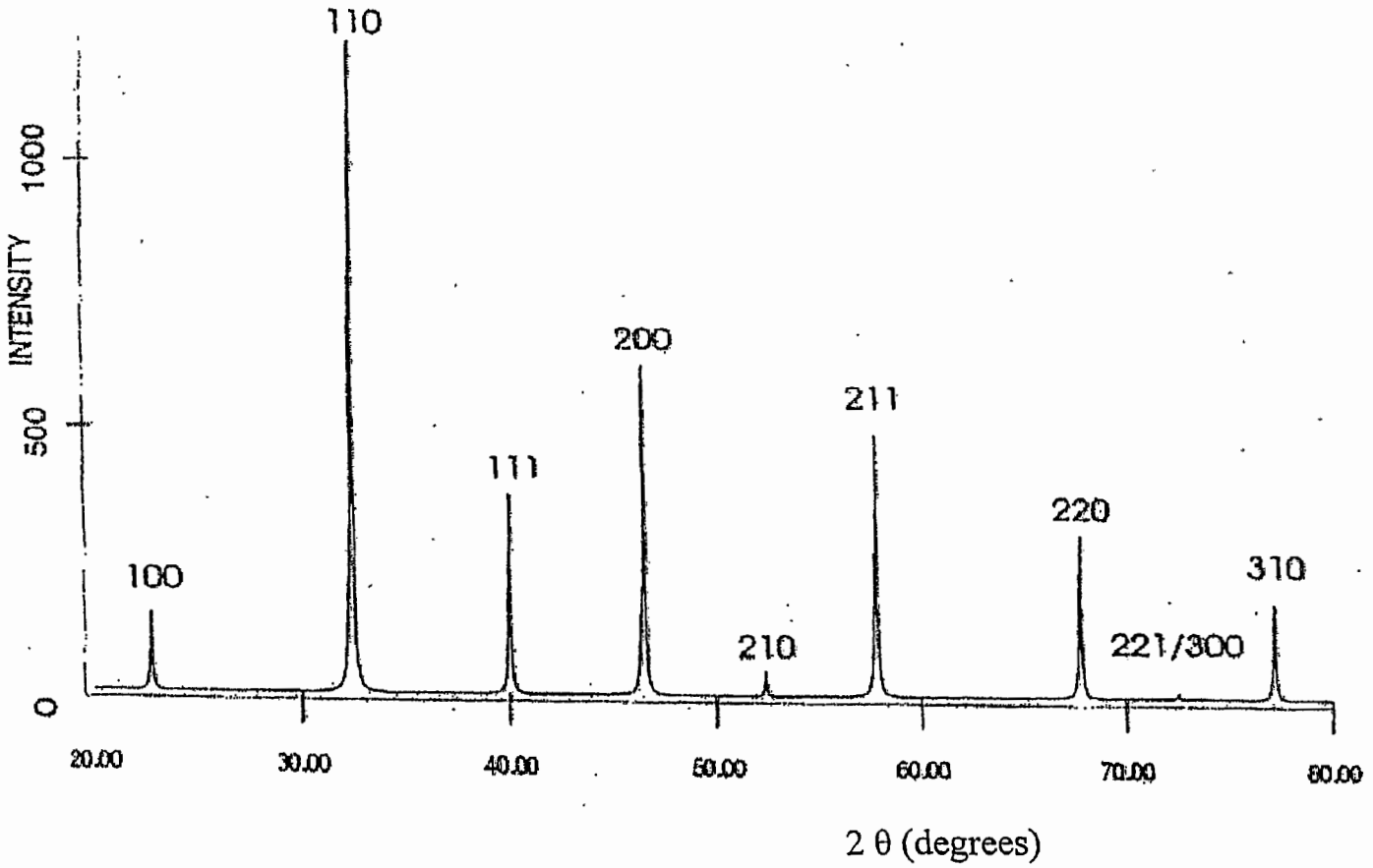

-Taken from reference 11

Heat capacity measurements were carried out on the sample using a Quantum Design Physical Property Measurement System (PPMS) with the heat capacity option installed. The PPMS system measures the heat capacity at constant pressure using a thermal relaxation technique. During the data collection, the pressure in the sample chamber was held to approximately 2mTorr or less during the entire measurement process. Although this pressure is relatively high for heat capacity determinations, a check was made to see how the heat capacity of a sample of high purity copper (99.999%, Kurt J. Lesker Co.), that was obtained using the same pressure condition in the system, compared with accepted Cu heat capacity data. The agreement of the two sets of data was very good. Consequently, the data in the study was taken to be acceptable. The high-pressure condition was later determined to be due to a vacuum leak into the sample chamber. When a leak detector became available, a vacuum check identified the leak and the problem was corrected. The pressure in the system now attains value near 9×10^{-5} Torr. During a heat capacity measurement, a known quantity of heat, ΔQ, is applied to the substrate on which the sample is mounted. The sample is in good thermal contact with the substrate and so it is heated also.

Over all the measurements, the sample and the substrate temperatures were very close as the "sample coupling" was between 93% and 99%. This coupling is defined on the next page. Hence, the change in the temperature of the

sample and the substrate was considered to be approximately the same during a measurement.

The total heat capacity C_{total}, which is measured, is

$$C_{total} = \Delta Q/\Delta T. \quad (3.1)$$

This total heat capacity includes not only the sample heat capacity, but in addition, it contains a non-sample component $C_{addenda}$ that is due to the heating of the platform (substrate) on which the sample is mounted, the electrical wires, and of other necessary components that are located on, or connected to, the substrate. Hence, C_{total} is given by the relation

$$C_{total} = C_{addenda} + C_{sample} \quad (3.2)$$

Before carrying out the heat capacity measurements of the sample, the addenda heat capacity $C_{addenda}$ is determined by performing heat capacity measurements of the sample holder, without the sample, over the temperature range to be used in the sample measurement. Thus, when the heat capacity measurements, with the sample installed, is performed, $C_{addenda}$ can be subtracted from C_{total} to yield C_{sample}. The heat capacity data were collected over the temperature range of 2 - 300 K in zero applied magnetic field.

The thermal connection between the sample and the substrate is referred to as the "sample coupling" in the PPMS data output, and it describes how good the thermal conductance is between the sample and the substrate. A sample coupling of 100% represents the best possible thermal conductance. For the heat capacity measurements, the sample coupling ranged from 93% at the highest

temperatures to 99% at the lowest temperatures. The addenda heat capacity that was measured in the study was of the order of a few μJ/K. The C_{sample} uncertainty was at a maximum of 8.1% at the highest temperatures and reduced to 1.1% at the lowest temperatures.

The PPMS heat capacity option calculates the heat capacity data using one of two different models. The "simple model" assumes that there is good thermal contact between the sample and the substrate, and the sample and sample platform are at the sample temperature. Heat transfer is assumed to be only between the substrate and the sample. The other model is the "two-tau model" which is used when there is relatively poor thermal contact between the sample and the sample platform. This model considers that the heat transfer takes place not only between the substrate and the sample but also between the substrate and the entire sample holder unit.

In this chapter, the heat capacity data are analyzed. Figure 4.1 shows a graph of the sample heat capacity data over the entire temperature range (2 K < T < 300 K). As shown in the graph, the heat capacity increases slowly from 2 K to around 20 K. The graph then increases linearly from about 30 K to near 120 K. Above 120 K, the slope of the graph begins to gradually decline, with C approaching a maximum near 0.54 J/g-K (or 222.13 J/mol-K) at a temperature of 300 K. The Dulong-Petit law predicts that at high temperatures, the heat capacity saturates at the Dulong-Petit value of 3nR, where n is the number of atoms per molecule of material and R is the universal gas constant, which has a value of 8.314 J/mol-K. For the material that was intended, $Ca_2EuZrO_{5.5}$, n = 9.5 and the Dulong-Petit law predicts a value of 0.58 J/g-K (or 236.95 J/mol-K) which is slightly different from the value obtained from the graph. No composition determination was performed on the sample because it disintegrated before the determination process could be done, and the sample has now returned to powder form.

The total heat capacity C of a material consists of various contributors including, the lattice or phonon heat capacity (C_{ph}), the electronic heat capacity (C_{elec}), the nuclear heat capacity (C_{nuc}), and in the case of magnetic materials, the magnetic heat capacity (C_{mag}). Thus, the total heat capacity of a material can be expressed as[6]

$$C = C_{ph} + C_{elec} + C_{nuc} + C_{mag} + C_i \tag{4.1}$$

Figure 4.1:
C vs. T of the Sample
for 2 K - 300 K

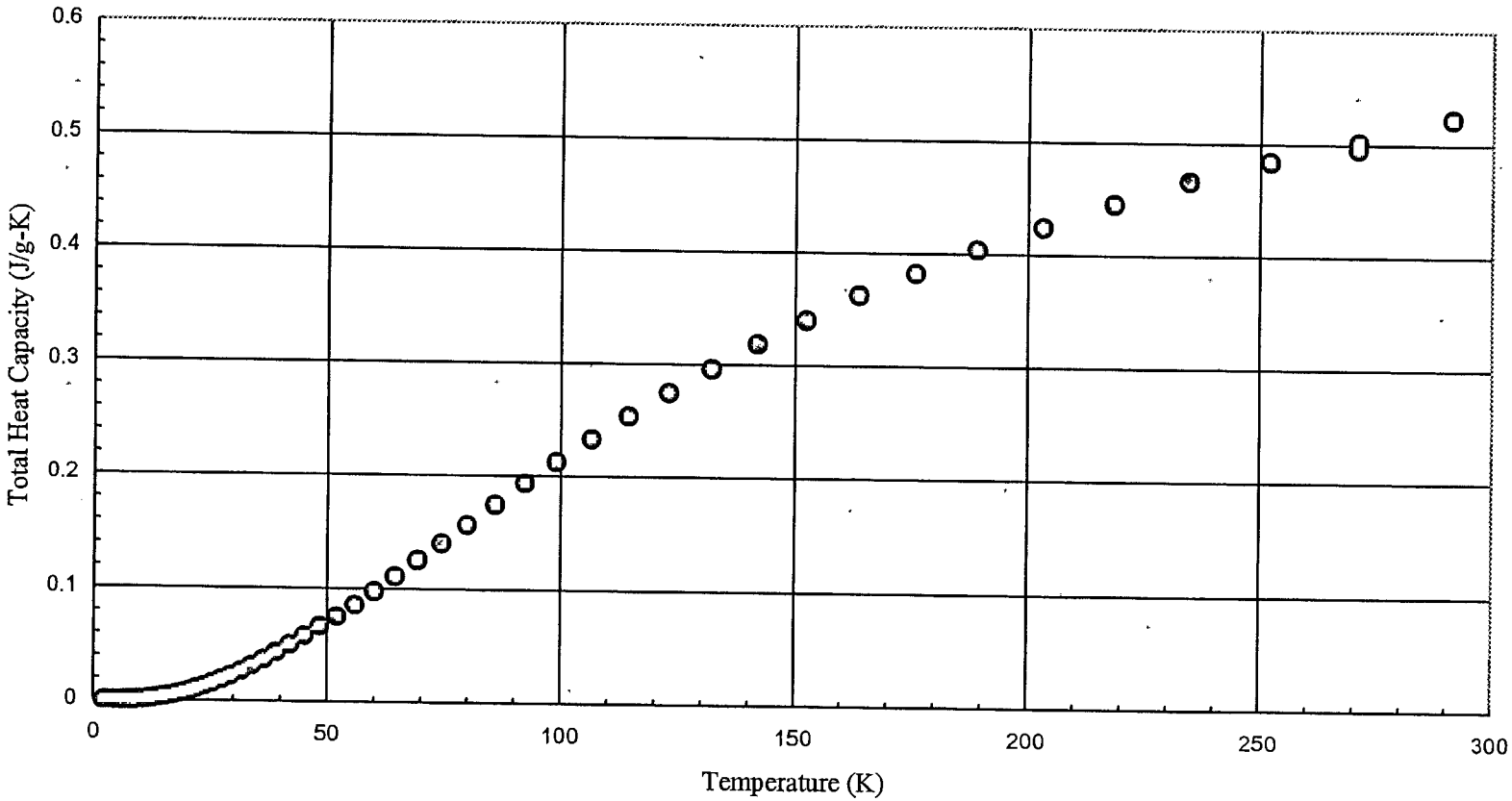

where C_i represents any additional contributors. Typically, for metals, the first four terms are dominant. The first three terms can be determined independently from their relative strengths in various temperature ranges due to their different temperature dependencies. Since the PCO based alloy sample is non-magnetic and the heat capacity measurements were done above 2 K, both the nuclear and magnetic terms will be neglected. (The nuclear contribution becomes dominant at very low temperatures, i.e., $T < 2$ K). Mathematically, the temperature dependence of the remaining contributors is stated as follows

$$C_{elec} = \gamma T \tag{4.2}$$

and

$$C_{ph} = \alpha T^3 \tag{4.3}$$

where γ and α are constants to be determined. Consequently, C is given by

$$C = \gamma T + \alpha T^3. \tag{4.4}$$

By plotting the heat capacity versus various temperature scales, the constants (α and γ) and subsequently the individual contributors (C_{ph} and C_{elec}) to the total heat capacity can be determined.

The constant γ is related to the Fermi temperature of the material by the relation[7]

$$\gamma = (9nN_Ak_B/2T_F), \tag{4.5}$$

where n is the number of atoms per molecule, N_A is Avogadro's number (6.026×10^{23} molecules/mol), k_B is Boltzmann's constant (1.38×10^{-23} J/K) and T_F is the Fermi temperature. T_F is given by the equation

$$T_F = E_F/k_B, \quad (4.6)$$

where E_F is the Fermi energy. The constant γ is also related to the density of states, $DOS(E_F)$, at the Fermi level by the relation

$$\gamma = (\pi^2/3)DOS(E_F)k^3_B. \quad (4.7)$$

$DOS(E_F)$ gives the population of electrons at the Fermi level. For temperatures below $1/10^{th}$ the Debye temperature θ_D, the constant α is given by[8]

$$\alpha = (12rR\pi^4/5\theta_D^3). \quad (4.8)$$

Here, r is the number of atoms per molecule and R is the universal gas constant.

In order to identify the various heat capacity contributors of the sample, the data are expanded in the temperature range from 2 K - 20 K. This expansion is shown in Figure 4.2. The heat capacity increases slowly at the lowest temperatures, and then the slope gradually increases.

Starting estimates of the electronic and lattice heat capacity coefficients will now be obtained. Rewriting equation 4.4 as[9]

$$C/T = \gamma + \alpha T^2 \quad (4.9)$$

Figure 4.2:
C vs. T of the Sample
for T < 20 K

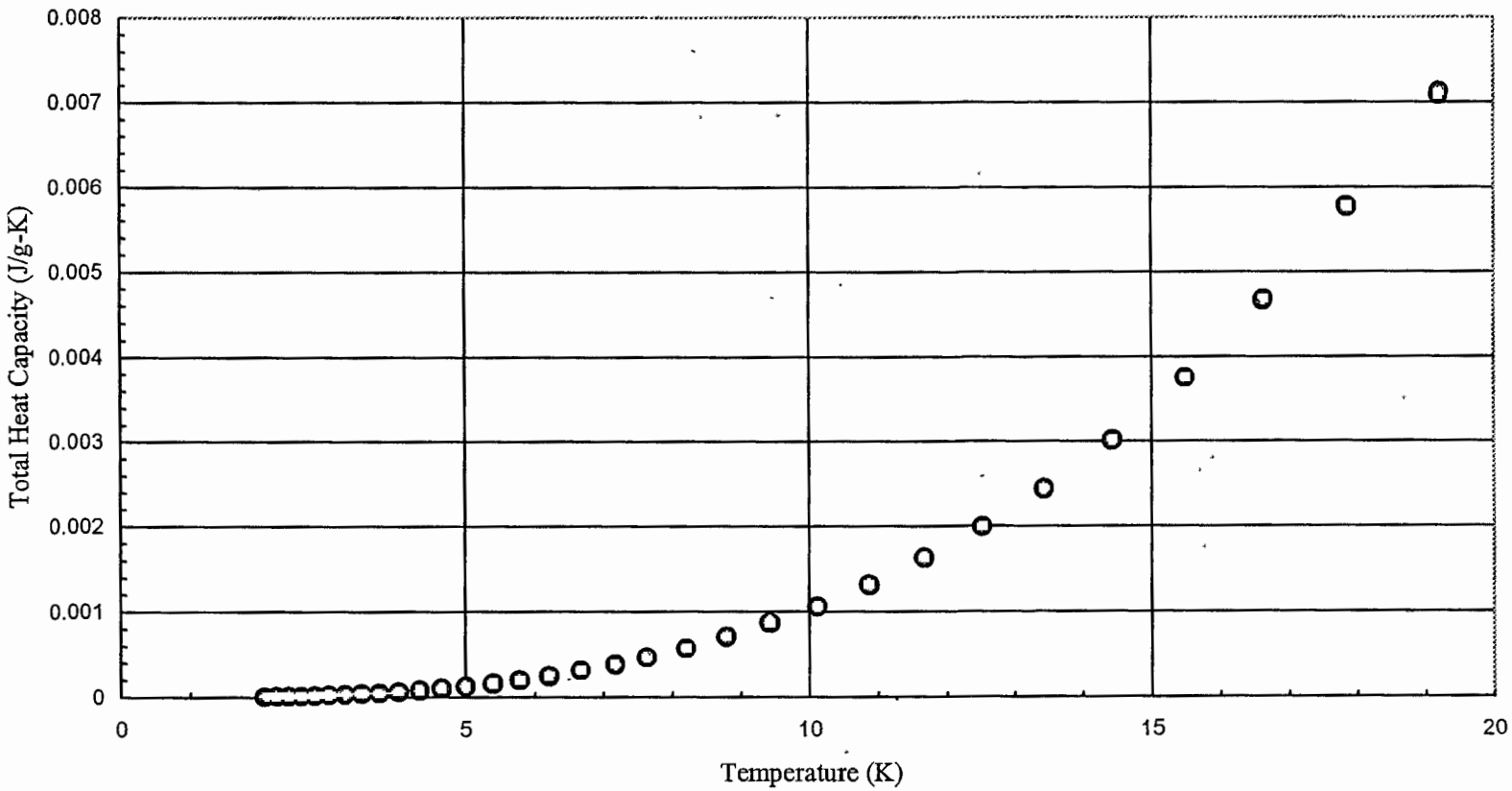

suggests that plotting a graph of C/T vs. T^2 will allow determination of the values of γ (the C/T-intercept) and α (the slope) for the electronic and lattice heat capacity coefficients, respectively.

Figure 4.3 is a plot of C/T vs. T^2 over the temperature range from 2 K < T < 4 K. The data produce a straight line. Using Microsoft Excel, a linear fit of the data yielded values of the C/T-intercept of 2×10^{-7} J/g-K^2 and a slope of 1×10^{-6} J/g-K^4 as values for γ and α, respectively. A plot of the data were made over a larger temperature range (2 K < T < 20 K). As expected, in light of the shape of the curve from 2 – 20 K, no fit to the straight line could be found.

Recalling that γ is the coefficient of the electronic heat capacity and using $\gamma = 2 \times 10^{-7}$ J/g-K^2, estimates of the density of states $DOS(E_F)$ and the Fermi energy (E_F) of the material can be made. Hence, using equation 4.7[10],

$$DOS(E_F) = (3\gamma/\pi^2 k^2_B) \qquad (4.10)$$

and the electron density of states at E_F is 5.113×10^{19} electrons/g-eV. Since equations 4.5 and 4.7 are equivalent, they can be used to solve for $DOS(E_F)$. From equations 4.5 and 4.7

$$9nN_A k_B/2T_F = (\pi^2/3)DOS(E_F)k^2_B. \qquad (4.11)$$

Rewriting equation 4.11, using equation 4.6, and approximating $\pi^2/3$ as equal to 3 leads to

$$9nN_A k_B/2E_F \cong 3DOS(E_F)k_B^2. \qquad (4.12)$$

Figure 4.3:
C/T vs. T^2 of the Sample
for T < 4 K

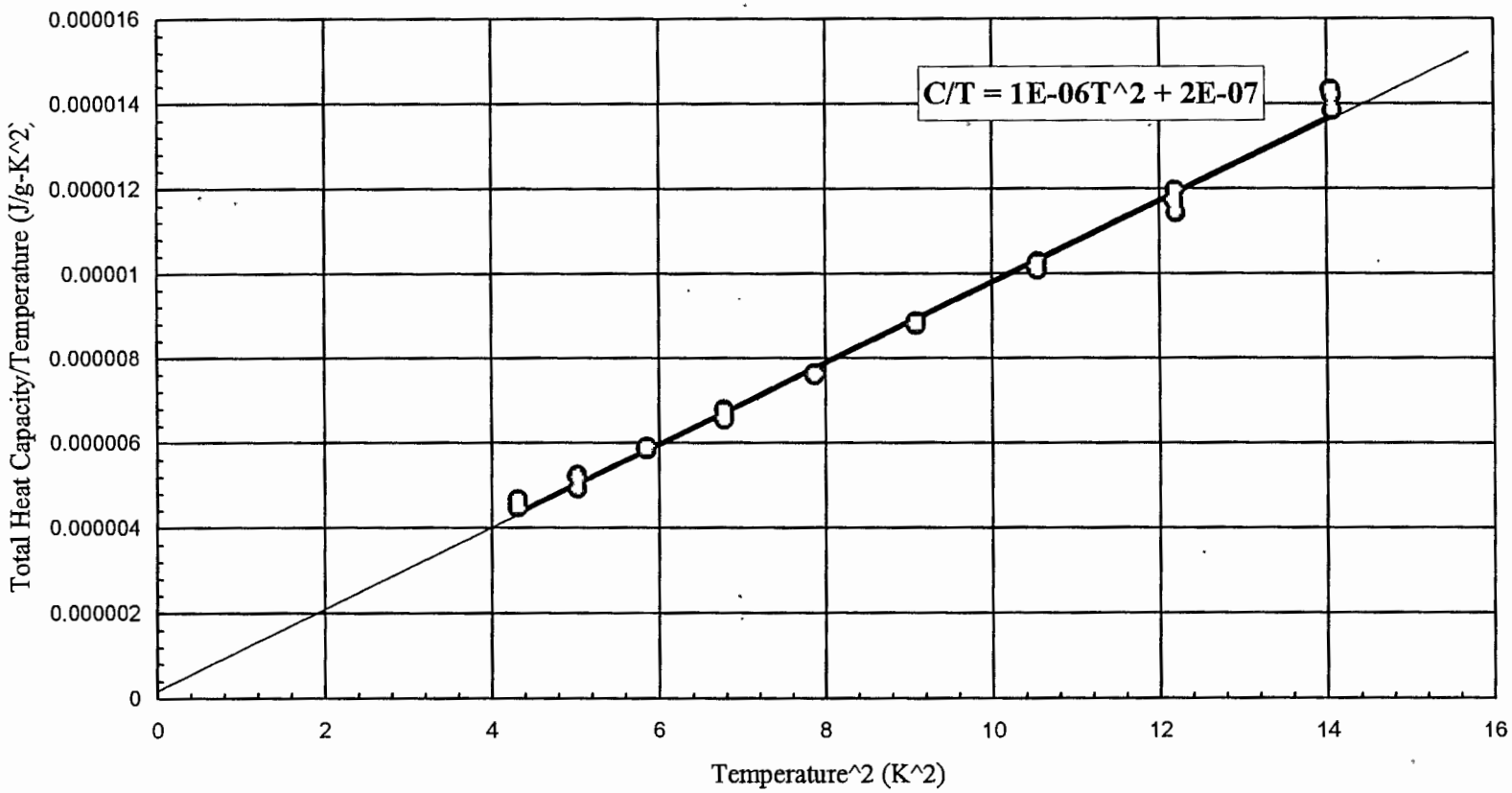

This approximation is done to obtain estimates for E_F and T_F. The approximation of $\pi^2/3 = 3$ results in a 10% error for the values of E_F and T_F. Solving for DOS(E_F) gives[10]

$$DOS(E_F) \cong 3nN_A/2E_F. \tag{4.13}$$

The Fermi energy is then[10]

$$E_F \cong 3nN_A/2DOS(E_F), \tag{4.14}$$

giving a value of $E_F \cong 406.90 \pm 10\%$ eV. Knowing E_F and using equation 4.6, the Fermi temperature yields a value of $4.72 \times 10^6 \pm 10\%$ K.

Using the values obtained for α and γ, plots for the lattice and electronic heat capacities are made. On a graph of heat capacity versus temperature, the electronic heat capacity is linear and the lattice heat capacity rapidly increases. This is shown in Figures 4.4 and 4.5. As seen in Figure 4.6, the lattice heat capacity is dominant in the 2 K – 20 K temperature range.

Now that the electronic and lattice heat capacity contributions are calculated, they can be compared with values calculated from the theory by calculating lattice heat capacity coefficient α and using it to solve for the electronic heat capacity coefficient γ. This can be done using equation 4.8 and solving for α. Doing this gives the results that

$$\alpha = 12\pi^4 rR/5\theta_D^3 \tag{4.15}$$

$$= 12\pi^4(9.5)(8.314 \text{ J/mol-K})/5(407.27 \text{ K})^3$$

$$= 2.73 \times 10^{-4} \text{ J/mol-K}^4$$

$= 6.64 \times 10^{-7}$ J/g-K^4.

Table 4.1 gives a summary of the estimates for the coefficients of the heat capacity contributors and values of some related parameters.

Figure 4.4:
C(ph) vs. T of the Sample
for T < 20 K

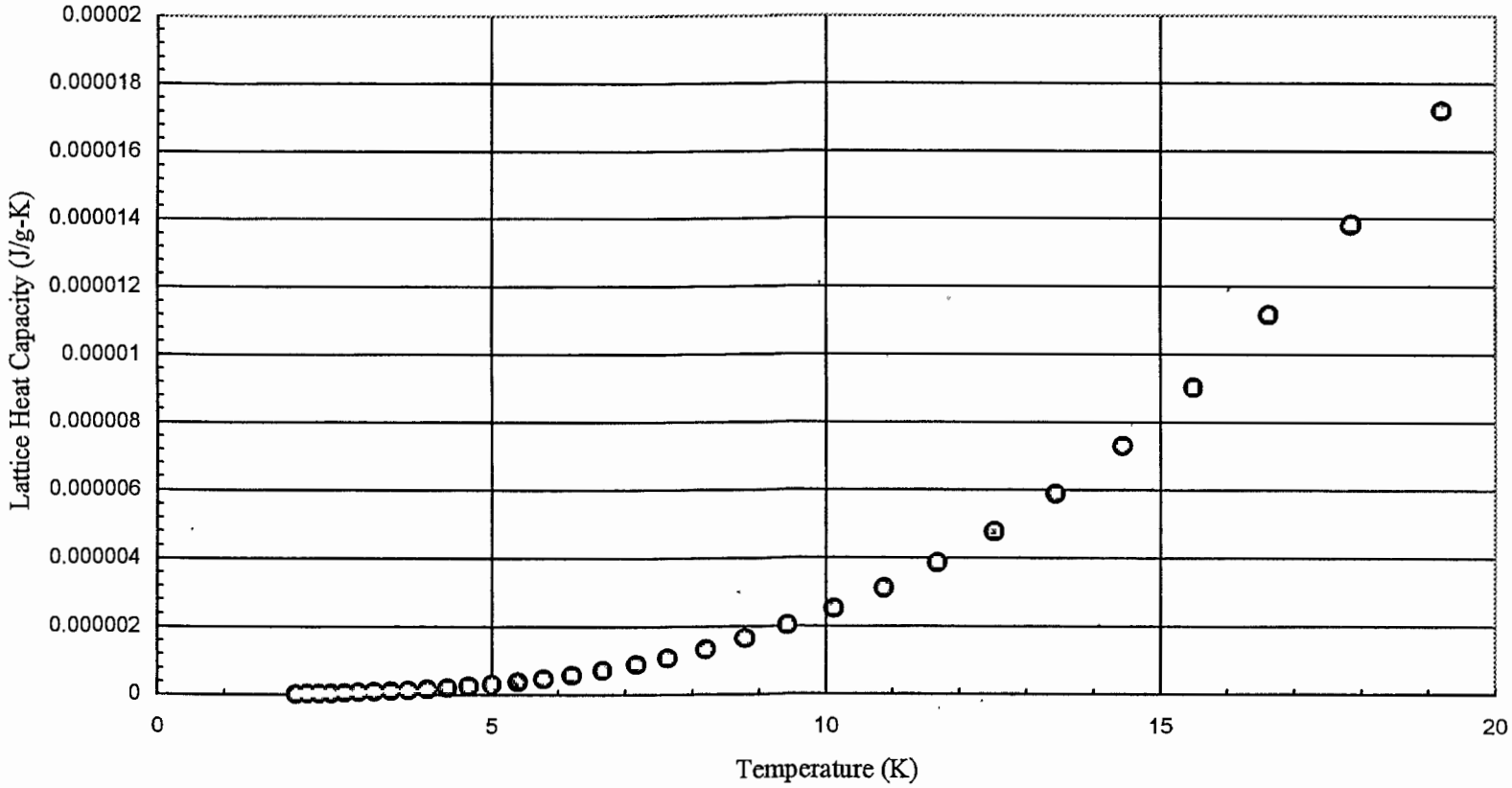

Figure 4.5:
C(elec) vs. T of the Sample
for T < 20 K

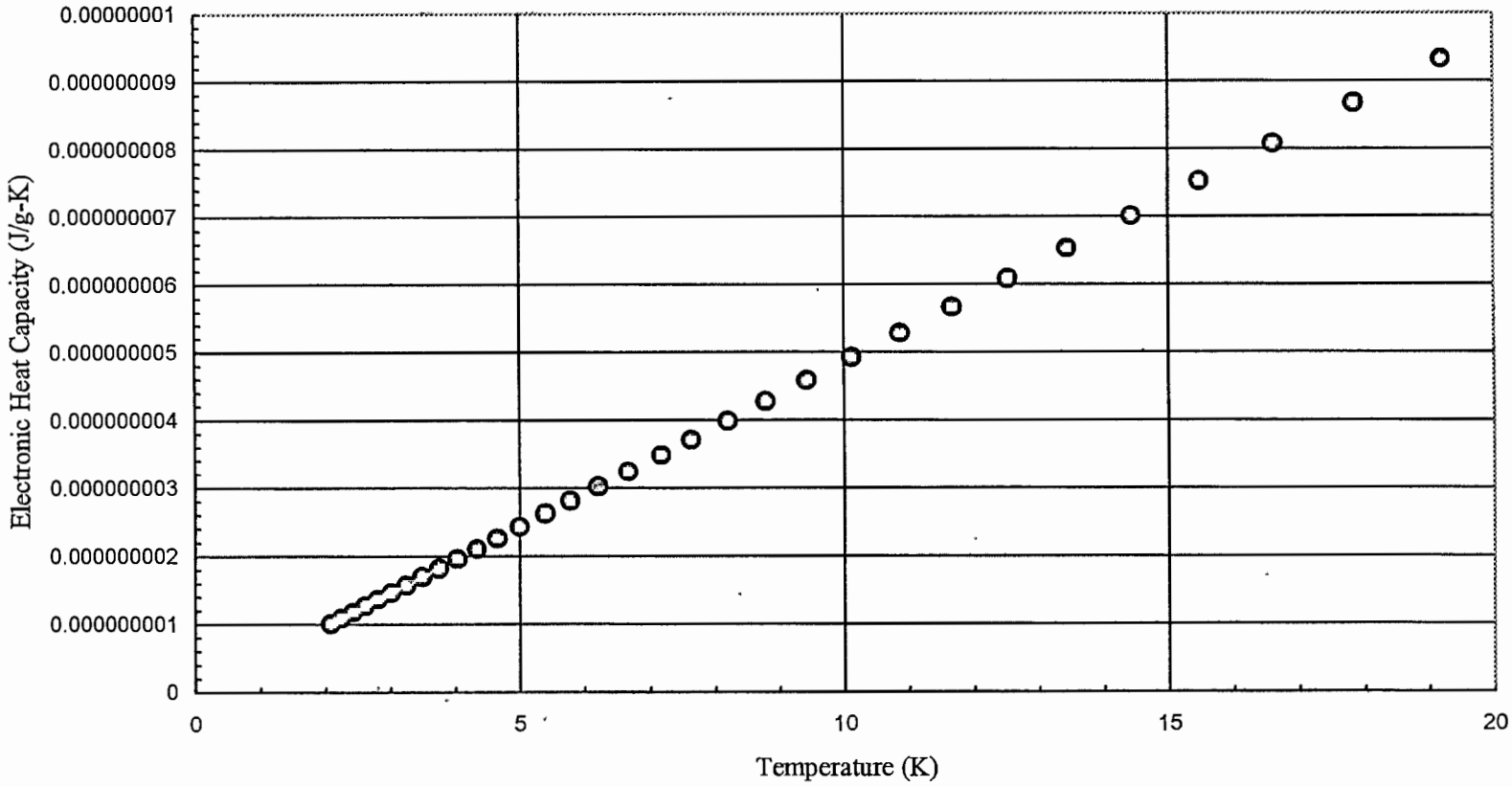

Figure 4.6:
C(ph) and C(elec) vs. T of the Sample
for T < 8 K

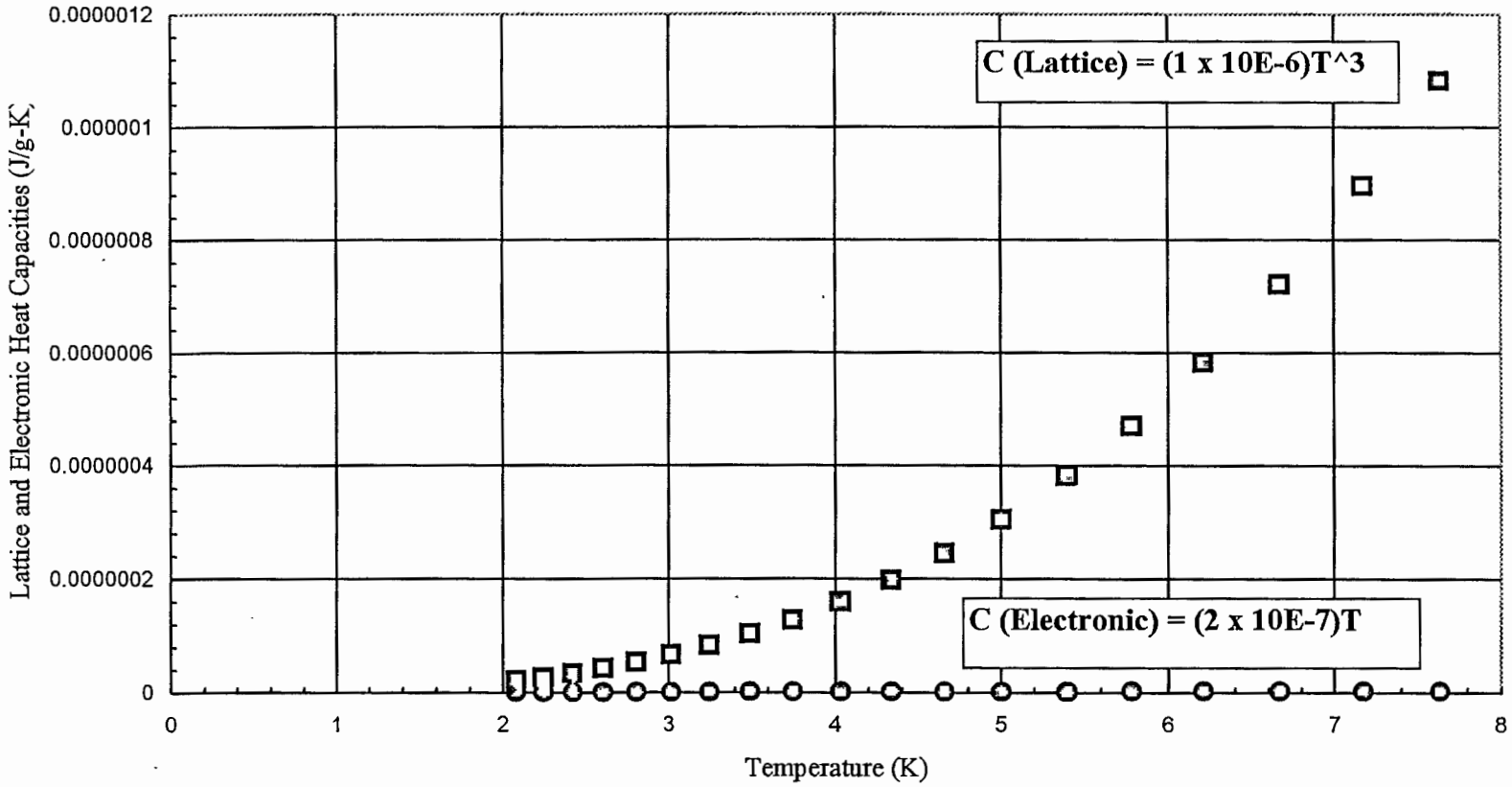

Chapter 5: Conclusion

In conclusion, the calorimetric properties of a CaEuZrO based alloy sample were investigated by analyzing low temperature (2 K < T < 20 K) heat capacity data. On a plot of total heat capacity versus temperature, the heat capacity appeared to approach a maximum near 0.54 J/g-K (or 222.13 J/mol-K) at a temperature just above 300 K. This value is slightly less than that of the predicted Dulong-Petit value, which implies that the sample made was not the desired $Ca_2EuZrO_{5.5}$. Estimates of the constants α and γ and subsequently the individual contributors (C_{ph} and C_{elec}) to the total heat capacity were determined by plotting the heat capacity data versus various temperature scales. The lattice and electronic heat capacity coefficients were determined to be 1×10^{-6} J/g-K^4 and 2×10^{-7} J/g-K^2, respectively. Thus, the lattice heat capacity was shown to be dominant from 2 K to 20 K. As shown in Figure 4.6, the lattice heat capacity dominates the total heat capacity in the 2 K - 20 K temperature range. Using γ, we made estimates of the electron density of states (at E_F) and of the Fermi energy of the sample. The values were calculated to be 5.113×10^{19} electrons/g-eV and 406.90 ± 10% eV, respectively. Using the Fermi energy, the Fermi temperature was calculated to be 4.72×10^6 ± 10% K. These values for the coefficients of the heat capacity contributors and related parameters are given in Table 4.1.

Bibliography

1. R. Jose, J. James, Asha John, R. Divakar, and J. Koshy, "Synthesis and Characterization of nanoparticles of $Ba_2EuZrO_{5.5}$: A new complex perovskite ceramic oxide," Journal of Materials Research, Volume 15, October 2000, pg. 2125 – 2130.

2. R. Jose, J. James, Asha John, R. Divakar, and J. Koshy, "Synthesis and Characterization of nanoparticles of $Ba_2EuHfO_{5.5}$: a new complex perovskite ceramic oxide," Materials Letters, Volume 51, Issue 3, November 2001, pg. 275 – 280.

3. R. Jose, J. James, Asha John, R. Divakar, and J. Koshy, "Synthesis of nanosized $Ba_2LaZrO_{5.5}$ ceramic powders through a novel combustion route," Journal of Materials Synthesis and Processing, Volume 8, Issue 1, January 2000, pg. 1-5.

4. R. Jose, J. James, Asha John, R. Divakar, and J. Koshy, "Barium holmium zirconate, a new perovskite oxide: II, synthesis as nanoparticles through a modified combustion process," Journal of the American Ceramic Society, Volume 85, Issue 10, October 2002, pg. 2395-2398.

5. R. Jose, Asha M. John, J. James, K.V.O. Nair, K. V. Kurian, J. Kosy, "Superconducting Bi (2223) films ($T_c(0)$ = 100 K) by dip-coating on $Ba_2LaZrO_{5.5}$: a newly developed perovskite ceramic substrate," Materials Letters, Volume 41, November 1999, pg. 112 – 116.

6. Laurence L. Henry, Ph.D., Introduction to Materials Characterization (Magnetization, I-V, and Heat Capacity Techniques), 2000, pg. 73-74.

7. Wert and R. Thomson, Physics of Solids, 2nd ed. (McGraw-Hill, Inc., 1964), pg. 36-41, 182-183, 222-226.

8. E.S.R. Gopal, Specific Heats at Low Temperatures, (Plenum Press, New York, 1966), pg. 5, 20-22, 25-31, 55-61, 90-92.

9. C. Kittel, Introduction to Solid States Physics, 4th ed. (John Wiley & Sons, Inc., 1971), pg. 249-255.

10. Richard Turton, The Physics of Solids, (Oxford University Press, 2000), pg. 200-202.

11. Mark T. Weller, Inorganic Materials Chemistry, (Oxford Science Publications, 1996), pg. 40.

12. D. Halliday, R. Resnick, J. Walker, Fundamentals of Physics, 4th ed., (Wiley, 1993).

13. R.F. Patterson, New Webster's Dictionary, 1993 edition, (P.S.I. & Associates, 1992).

14. P.V.E. McClintock, D.J. Meredith, and J.K. Wigmore, Matter at Low Temperatures, (New York: Wiley 1984).

15. H. M. (Harold Max) Rosenberg, Low Temperature Solid State Physics; Some Selected Topics, (Oxford, Clarendon Press, 1963).

16. A.F. Clark, R. P. Reed and G. Hartwig, Nonmetallic Materials and Composites at Low Temperatures, (New York: Plenum Press, c1979).

17. D.A. Wigley, Mechanical Properties of Material at Low Temperatures, (New York, Plenum Press, 1971).

18. Richard A. Robie and Bruce S. Hemingway, Calorimeters for Heat of Solustion and Low-Temperature Heat Capacity Measurements, (Washington: U.S. Govt., Print Off., 1972).

19. Frank Pobell, Matter and Methods at Low Temperatures, (Berlin; New York; Springer-Verlag, c1992).

20. L. (Lachlan) MacKinnon, Experimental Physics at Low Temperatures; An Introductory Survey, (Detroit, Wayne States University Press, 1966).

21. Anthony Kent, Experimental Low Temperature Physics, (New York: American Institute of Physics, 1993).

22. O.V. Lounasmaa, Experimental Principles and Methods Below 1K, (London; New York: Academic Press, 1974).

23. Y.S. Touloukian and E.H. Buyco, Specific Heat: Metallic Elements and Alloys, (New York, IFI/Plenum, 1970).

24. W. Hemminger and G. Hohne (Translated by Y. Goldman), Calorimetry: Fundamentals and Practices (Weinheim; Deerfield Beach, Florida: Verlag Chemge, c1984).

25. A.A. Maradudin et al., Lattice Dynamics, (New York, Benjamin, 1969).

26. H. M. (Harold Max) Rosenburg, The Solid State: An Introduction to the Physics of Crystals for Students of Physics, Material Science, and Engineering, 2nd ed. (Oxford: Clarendon Press, 1988).

27. Joan Warnon-Blewett and Jurgen Teichmann, Guide to Sources for History of Solid State Physics, (New York: Center for History of Physics, American Institute of Physics, 1992).

Vita

Ms. Watasha M. Wade was born in Baton Rouge, Louisiana on November 11, 1973. She graduated from Scotlandville Magnet High School in May of 1991. In the fall of 1991, Ms. Wade enrolled in Southern University and A & M College (Baton Rouge), where she received a Bachelor of Science degree in physics in the fall of 1995. Watasha entered the M.S. Physics Program in the fall of 1996 and worked as a teaching assistant at Southern University Laboratory School while pursuing her degree. After working in corporate America for several years, Ms. Wade returned to complete her degree.

APPROVAL FOR SCHOLARLY DISSEMINATION

The author grants to the Southern University Library the right to reproduce, by appropriate methods, upon request, any or all portions of this thesis.

It is understood that "request" consists of the agreement on the part of the requesting party, that said reproduction is for his personal use and the subsequent reproduction will not occur without written approval of the author of this thesis.

The author of this thesis reserves the right to publish freely, in the literature, at any time, any or all portions of this thesis.

Author Natasha M. Wade

Data 14/9/03